Separating polymer solutions with supercritical fluids

4 AUTHORS, INCLUDING:

Mark A Mchugh
Virginia Commonwealth University
194 PUBLICATIONS **4,885** CITATIONS

in model I (eq 8) to be $K = 184$ kJ mol^{-1} nm^{-2}. Taking values of the lattice spacings l_α and l_β in the two phases from ref 4 and 12, we set $l_\alpha = 1.16$ nm and $l_\beta = 1.30$ nm. The mean-field prediction for ΔF (eq 14) is shown as the solid line in Figure 2. We see that the mean-field prediction lies close to the experimental result.

Figure 3 shows the behavior of the stress–strain curves obtained from the mean-field approximation to model I, i.e., the stable and metastable solutions to eq 7. The considerable hysteresis predicted at low temperatures diminishes with increase in temperature, vanishing at the critical point. In plotting Figure 3, we took the values of the conformational energies E_α and E_β from the calculation of Yokouchi et al.,[6] who found $E_\alpha = -6.60$ kJ mol^{-1} and $E_\beta = -1.21$ kJ mol^{-1}, and the stress F expressed per unit polymer backbone was divided by the average cross-sectional area of a unit cell (taken to be 0.28 nm^2) in order to convert it to conventional units.

Figure 4 is a plot of the stress–strain curves for model II at one temperature below T_c and at one temperature above T_c. The parameter V_0 appearing in model II was fixed by requiring that the critical temperature equal 415 K. This leads to a value of V_0 equal to -3.34 kJ mol^{-1}.

Although model II is considerably more complex than model I, it nevertheless also has the character of a mean-field model and yields similar values for the critical exponents. We thus find that model II also produces a straight-line plot in Figure 2, where points from the Monte Carlo simulations are shown as open circles. The slope of this line, however, is in considerably poorer agreement with experiment than is the case for model I.

The highly simplified models of PBT that we have studied allow us to understand qualitatively the nature of the atomic displacements during the α–β structural transition. The results presented here show that model I yields better agreement with experiment than model II, sug-

gesting that benzene rings from neighboring chains remain in registry during the transition.[13] In future work, we propose to refine these models to include the structure of the tetramethylene segment and to take into account more realistic van der Waals interactions between benzene rings.

References and Notes

(1) B. Stambaugh, J. B. Lando, and J. L. Koenig, *J. Polym. Sci., Polym. Phys. Ed.*, **17**, 1063 (1979).
(2) M. G. Brereton, G. R. Davies, R. Jakeways, T. Smith, and I. M. Ward, *Polymer*, **19**, 17 (1978).
(3) K. Tashiro, Y. Nakai, M. Kobayashi, and H. Tadokoro, *Macromolecules*, **13**, 137 (1980).
(4) Z. Menzik, *J. Polym. Sci., Polym. Phys. Ed.*, **13**, 2173 (1975).
(5) B. Stambaugh, J. L. Koenig, and J. B. Lando, *J. Polym. Sci., Polym. Phys. Ed.*, **17**, 1053 (1979).
(6) M. Yokouchi, K. Sakakibara, Y. Chatani, M. Tadokoro, T. Tanaka, and Y. Yoda, *Macromolecules*, **9**, 366 (1976).
(7) W. Strohmeier and W. F. X. Frank, *Colloid Polym. Sci.*, **260**, 937 (1982).
(8) E. Ising, *Z. Phys.*, **31**, 253 (1925).
(9) H. N. V. Temperley in "Phase Transitions and Critical Phenomena", Vol. 1, C. Domb and M. S. Green, Eds., Academic Press, New York, 1972, p 227.
(10) K. Binder, Ed., in "Monte Carlo Methods in Statistical Physics", Springer, West Berlin, 1979, *Top. Curr. Phys.* Vol. 7.
(11) N. Metropolis, A. W. Rosenbluth, M. N. Rosenbluth, A. H. Teller, and E. Teller, *J. Chem. Phys.*, **21**, 1087 (1953).
(12) I. H. Hall and M. G. Pass, *Polymer*, **17**, 807 (1976).
(13) We would like to point out here that the conformational energy parameters appearing in the two models do not play a role in determining the widths of the hysteresis loops. The results presented above are therefore valid in spite of the uncertainties in the conformational energies. A refinement of the conformational energy calculations would however lead to a better prediction of the critical stress.

Separating Polymer Solutions with Supercritical Fluids

Mark A. McHugh*

Department of Chemical Engineering, University of Notre Dame, Notre Dame, Indiana 46556

Terry L. Guckes

Exxon Chemical Company, Florham Park, New Jersey ·07932. Received July 9, 1984

ABSTRACT: The high-pressure phase behavior of mixtures consisting of random poly(ethylene-*co*-propylene), a mixed organic solvent, and a light supercritical fluid additive is experimentally investigated. The amount and type of supercritical fluid additive (methane, ethylene, propylene, and carbon dioxide) have a dramatic effect on the shape and location of the phase border curves of the polymer solution. In particular it is demonstrated that the lower critical solution temperature (LCST) curve can be shifted by more than 100 °C to lower temperatures by introducing a supercritical fluid additive to the polymer solution. The effect of pressure, over a range of 2.76–31.02 MPa, on the LCST curve is also determined.

Introduction

The possibility of designing novel, energy-efficient separation processes using supercritical fluids (SCF's) has generated an increased number of high-pressure phase behavior studies within the past decade.[1,2] However, very little work has been done in applying SCF technology to the problem of separating polymer solutions. For certain solution polymerization processes an extremely costly process step occurs when the polymer is separated from its solvent. In some instances the cost of this separation can amount to approximately 10% of the final cost of the

product.[3] Currently, the most common technique for separating polymer from solvent is to devolatilize the solvent from solution by steam stripping. This type of separation technique can be very energy intensive since the solvent can amount to 90–95% (w/w) of the solution.

Inducing a polymer–solvent phase split offers an alternative to steam stripping as a separation technique.[3–6] This phase splitting technique is based on the experimental observation first made by Freeman and Rowlinson[7] that a miscible polymer solution will split into two liquid phases if the system temperature approaches the critical tem-
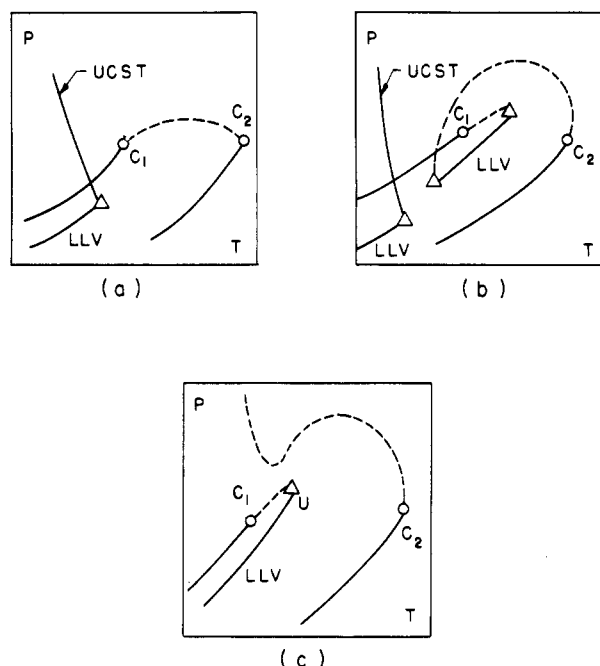
Figure 1. Pressure–temperature diagrams for three classes of binary mixtures.[17]

Figure 2. Representative $P-T$ diagram for polymer–solvent mixtures.

perature of the solvent. The phase separation, which is a consequence of the chemical nature of the components, their molecular sizes, especially the molecular weight of the polymer, and the critical temperature (T_c) and critical pressure (P_c) of the solvent,[8] occurs at the lower critical solution temperature (LCST). If the molecular weight of the polymer is on the order of 10 000, the LCST will occur within approximately 20–30 °C of the solvent's T_c. However, if the polymer molecular weight is extremely large, e.g., 10^6, the LCST can occur as low as 100 °C below the T_c of the solvent. It is shown in this work that introducing an SCF additive to the polymer solution can dramatically shift the LCST to lower temperatures and thus reduce the chances of thermally degrading the polymer.

Although a polymer–solvent mixture is in reality a multicomponent mixture due to the polydispersity of the polymer, the phase behavior of polymer solutions can be described by using the pressure–temperature $(P-T)$ diagram for binary mixtures such as those shown in Figure 1. These types of $P-T$ diagrams are used to explain the results of this study. Depicted in Figure 1a is the $P-T$ projection for a binary mixture where the two pure-component vapor–liquid equilibrium lines terminate at the pure-component critical points, C_1 and C_2. The dashed line represents the binary critical mixture curve which runs continuously from C_1 to C_2. Notice, however, that the liquids are not miscible at all temperatures. A liquid–liquid–vapor (LLV) line ending at an upper critical end point (UCEP) (i.e., a point at which one of the liquid phases becomes critically identical with the vapor phase in the presence of the other liquid phase) is now evident at temperatures lower than the critical temperature of either component. The upper critical solution temperature (UCST) line which begins at the UCEP and exhibits a slightly negative slope with increasing pressure represents the transition from two liquid phases to a single liquid phase with increasing temperature.

The type of phase behavior exhibited in Figure 1b is slightly more complicated than the previously described system. The branch of the critical mixture curve which starts at the critical point of the component with the higher critical temperature intersects a region of liquid immis-
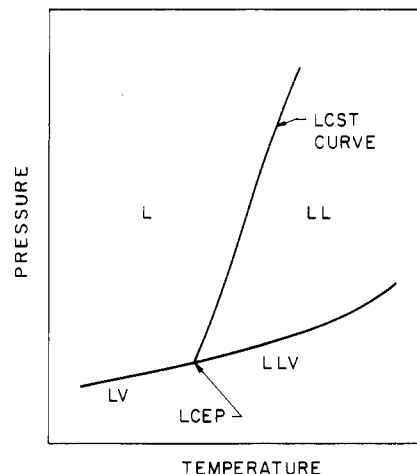
cibility at the lower critical solution temperature (LCST) (i.e., at the LCST the two liquid phases of the LLV line become critically identical in the presence of the vapor phase). The branch of the critical mixture curve which starts at the critical point of the other component intersects the LLV line at the UCEP. At temperatures below the LCST a region of liquid immiscibility again appears similar to that shown in Figure 1a.

Shown in Figure 1c is the $P-T$ projection for a binary mixture in which the components are very dissimilar in molecular size, shape, and/or polarity. In this instance the three-phase LLV line is intersected only once by the critical mixture curve at the UCEP. The other branch of the critical mixture curve which starts at the critical point of the heavier component never meets either the LLV line or the critical point of the lighter component.

Shown in Figure 2 is the section of the $P-T$ diagram for polymer–solvent mixtures which occurs very near the critical point of the solvent. This diagram is very similar to the section of the $P-T$ diagram near C_1 shown in Figure 1b. However, the LLV curve which is distinguishable from the solvent vapor pressure curve in Figure 1b is now projected onto the vapor pressure curve in the case of the polymer–solvent mixture in Figure 2. In this study we are mainly concerned with the branch of the critical mixture curve which intersects the solvent vapor pressure curve. We will follow the convention of Patterson[9] and call this part of the critical mixture curve the LCST curve and the intersection of the LCST curve with the vapor pressure curve the lower critical end point (LCEP). For polymer–solvent mixtures an UCST curve can also exist similar to those shown in Figure 1a,b.

Although inducing a polymer–solvent phase split as a means of separating polymer solutions offers certain advantages compared to steam stripping, one major disadvantage is that the polymer can thermally degrade at the high temperatures needed to induce the phase split. Irani et al.[10] addressed the problem of shifting the LCST curve to lower temperatures by introducing a light supercritical fluid as an additive to the polymer solution. To a first approximation the supercritical fluid lowers the critical temperature of the polymer solvent (now, in fact, a mixed solvent) and, hence, shifts the LCST curves to lower temperatures. As shown schematically in Figure 3, Irani et al.[10] found that the presence of the SCF additive shifts the phase boundary curves to lower temperatures without affecting the shapes of the curves.

Cowie and co-workers have previously investigated the phase behavior of polymer–mixed solvent systems. How-
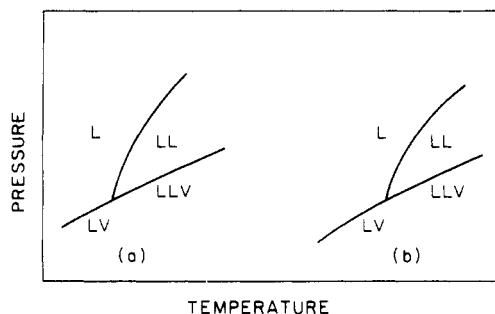
Figure 3. Schematic representation of the effect of an SCF additive on the phase boundary curves of a polymer–solvent mixture: (a) P-T projection of the phase boundary curves for a polymer–solvent mixture with an SCF added to the mixture; (b) same as part a but without the SCF additive.

Table I
Analysis of the EP Polymer and Solvent Used in This Study

Solvent

compd	concn, wt %
3-methylpentane	2.53
n-hexane	88.00
methylcyclopentane	9.45
other	0.02
	100.00

Poly(ethylene-co-propylene)[a]

$\bar{M}_n$	67000
$\bar{M}_w$	145000
$\bar{M}_w/\bar{M}_n$	2.2

42.8 wt % ethylene content

[a] By GPC analysis.

ever, their work is done at low pressures with the objective of studying cosolvent behavior.[11-14] The objective of this study is to investigate the high-pressure phase behavior of polymer solution–SCF mixtures. We are explicitly interested in determining the effect of an SCF additive on the phase border curves of polymer solutions. The polymer used in this study is a random poly(ethylene-co-propylene) (EP). The polymer solvent is a mixture of 3-methylpentane, methylcyclopentane, and n-hexane (see Table I). This composition of polymer solvent is representative of the type of solvent makeup used in a typical polymerization process. The supercritical fluids used as additives are methane, propylene, ethylene, and carbon dioxide.

Experimental Section

Shown in Figure 4 is a schematic diagram of the experimental apparatus used in this study. The apparatus and the experimental procedures are described in detail elsewhere[15] and, therefore, is only briefly described here. The supercritical fluid of interest is compressed and delivered to a holding tank located in a forced convection air bath. With valves 1 and 3 closed (see Figure 4) the pressure of the gas is measured with a Bourdon-tube Heise gauge to determine when the gas attains thermal equilibrium with the bath air. The gas is then transferred to the high-pressure view cell in which a measured amount of polymer solution has previously been charged. For these studies the concentration of polymer in the organic solvent (SCF-free basis) remains fixed at $5.24 \pm 0.1\%$ (w/w). The amount of gas transferred is determined by a mass balance based on the density of the gas remaining in the holding tank and the transfer lines and the volume of the tank and lines.

The variable-volume, high-pressure, view cell (316 stainless steel, 10.16 cm o.d. × 5.08 cm i.d., 250-cm³ working volume) is designed to operate to 34.47 MPa at 260 °C. The view cell is maintained at a constant temperature normally within ±0.1 °C. The cell contents, illuminated by a fiber light pipe, are viewed through a 2.54 cm thick, 7.00 cm diameter quartz window (Esco Products)
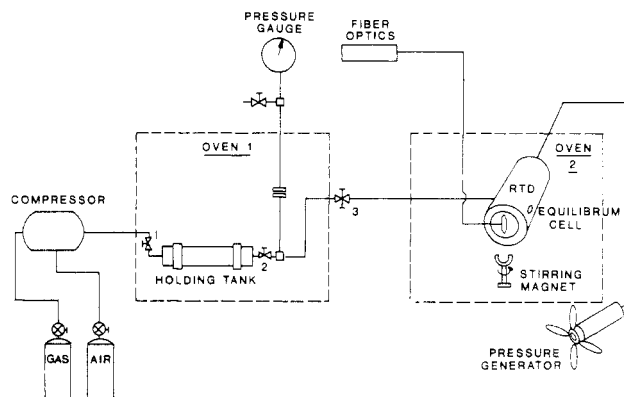

Figure 4. Schematic representation of the experimental apparatus used in this study to obtain the phase border curves for polymer–solvent–SCF systems.

which is secured by a cell end cap with a 0.64 cm by 5.08 cm view slit. The cell contents are mixed by a stirring bar activated by a magnet located below the cell. The contents can be compressed to the desired operating pressure by a movable piston. In this manner the pressure of the polymer mixture is adjusted at fixed overall composition by varying the mixture volume until the desired phase transition is observed.

Materials. The properties of the random poly(ethylene-co-propylene) (EP) are listed in Table I. Shown in Table I is an analysis of the polymer solvent used in this study. The ethylene (CP grade, 99.5% minimum purity), the propylene (CP grade, 99.0% minimum purity), the methane (CP grade, 99.0% minimum purity), and the carbon dioxide (bone dry grade, 99.8% minimum purity) were supplied by Linde Co. These components were used without further purification.

Experimental Procedure. Three types of phase border curves are determined in this study. They are the liquid + vapor → liquid curve, the liquid₁ + liquid₂ + vapor → liquid₁ + liquid₂ curve, and the liquid₁ + liquid₂ → liquid curve. The LCST phase border curves obtained in this study are actually cloud point curves (CPC's) since, for each experiment, the mixture composition remains fixed. However, Rowlinson and Myrat[16] and Zeman et al.[9] have shown that for the range of solution compositions used in this study the CPC is very close to the LCST curve. The technique for determining each of these phase border curves is described below.

Liquid + Vapor → Liquid Curve. Initially both vapor and liquid are present in the view cell. While vigorous mixing is maintained, the system pressure is increased at a constant temperature until the final bubble of vapor disappears. With a single liquid now in the view cell, the system pressure is slowly decreased until a small vapor bubble appears. The pressure at which the small vapor bubble appears when the mixture is decompressed is taken as the bubble point pressure.

Liquid₁ + Liquid₂ + Vapor → Liquid₁ + Liquid₂ Curve. The experimental technique in this case is similar to that for the liquid + vapor to liquid case; however, now there are two liquid phases present throughout the experiment. Also, the two liquid phases are generally opaque and grayish as opposed to the previous case where the single liquid phase is very clear. In fact, the heavier of the two liquid phases appears gellike, indicating that this phase is very rich in polymer.

Liquid₁ + Liquid₂ → Liquid Curve. Initially two grayish liquids are present in the view cell. While vigorous mixing is maintained at a constant temperature, the system pressure is isothermally increased until the two grayish liquids merge into a single clear liquid. Near the CPC curve the single liquid phase typically exhibits a light orangish hue. With a single liquid now in the view cell the pressure is slowly decreased until the liquid phase begins to become cloudy. The onset of turbidity is taken as the liquid → liquid + liquid phase transition. The pressure for this transition is defined as being in the interval between a single clear (orangish) phase in the cell and a cloudy cell condition which is completely opaque and where a meniscus separating the two liquid phases may or may not be discernible after approximately 10 min without mixing.
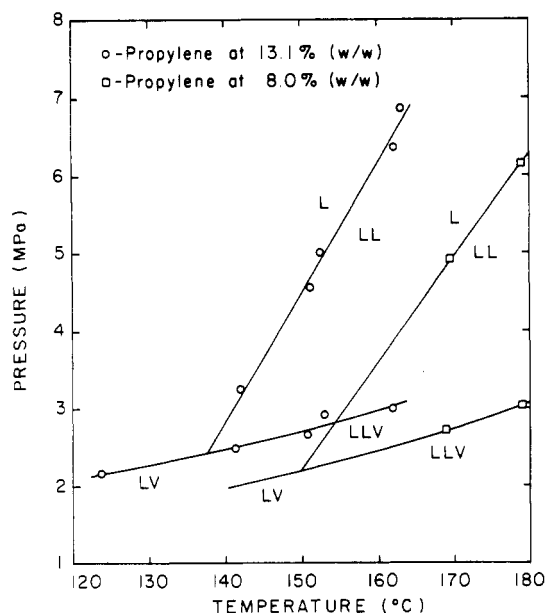
Figure 5. Phase border curves for the EP–solvent–propylene system at concentrations of 13.1% and 8.0% (w/w) propylene.

Results

The $P–T$ projections of various EP–solvent–SCF transition curves are shown in Figures 5–11 for supercritical propylene, ethylene, carbon dioxide, and methane. Since the primary focus of this study is to determine the effect of an SCF additive on the LCST curve of polymer solutions, no attempt is made to locate the UCST curve for these systems.

Shown in Figure 5 are the experimental $P–T$ data for the EP–solvent–propylene system at 13.1 and 8.0 wt % propylene. (These weight percents are based on the total weight of the solution. Tables of the experimental $P–T$ data for these and the other systems are provided as supplementary material. See the paragraph at the end of the text regarding supplementary material.) Without any propylene added to the polymer solution the phase border curves depicted in this figure are shifted to approximately 40–50 °C higher temperatures. The transition curves for the 13.1 wt % propylene system are similar to those at 8.0 wt %; however, they are shifted by approximately 15 °C to lower temperatures. For both of these systems and for the other systems subsequently discussed in this paper the LCEP is determined as the intersection of the LCST curve and the vapor pressure curve.

The EP–solvent–ethylene systems at 9.9, 13.8, and 20.0 wt % ethylene are shown in Figure 6. Compared to propylene, ethylene shifts the transition curves to much lower temperatures, but ethylene also shifts the vapor pressure curves to higher pressures. As shown in Figure 6, concentrations of ethylene of up to 20.0 wt % do not affect the shape of the transition curves. The slopes of the LCST curves for the ethylene and propylene systems are approximately equal at the loadings shown in Figures 5 and 6. These slopes are similar to the values obtained by Zeman et al.[9] for the LCST curves of the polystyrene–methyl acetate system.

The results of the determination of the $P–T$ projection of the EP–solvent–carbon dioxide (13.5 wt %) system are shown in Figure 7. These curves exhibit characteristics which are very similar to those of the propylene and ethylene systems; however, the vapor pressure curve for the CO_2 system is at higher pressures. The slope of the LCST curve is very close to those of the previously mentioned propylene and ethylene cases.
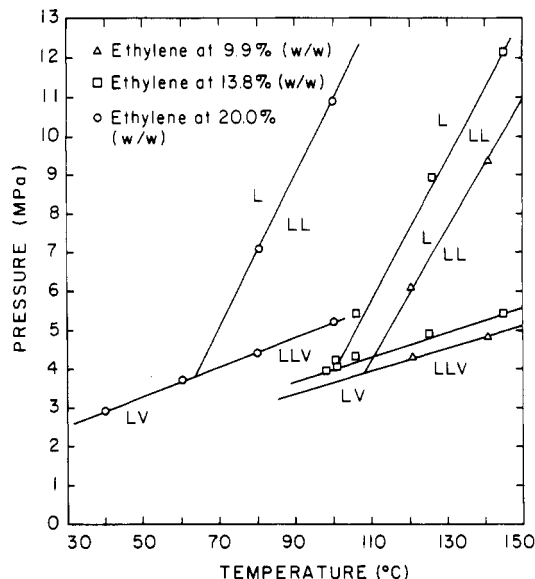

Figure 6. Phase border curves for the EP–solvent–ethylene system at concentrations of 9.9%, 13.8%, and 20.0% (w/w).
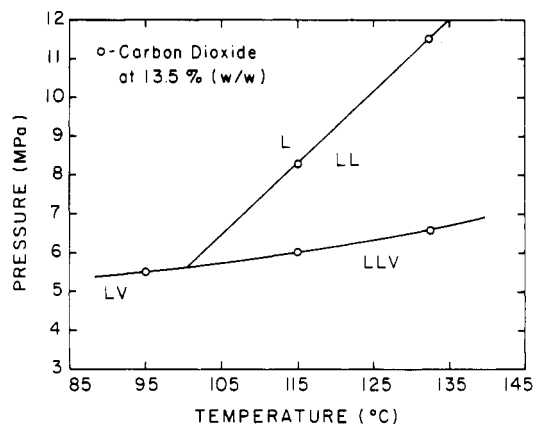

Figure 7. Phase border curves for the EP–solvent–carbon dioxide (13.5% (w/w)) system.

The $P–T$ behavior for the propylene, ethylene, and carbon dioxide systems at approximately the same loadings is shown in Figure 8. Compared to propylene, ethylene shifts the transition curves to lower temperatures; however, it also shifts the curves to higher pressures. Carbon dioxide shifts the curves to slightly lower temperatures than ethylene, but it also shifts the curves to higher pressures than ethylene.

Shown in Figure 9 is the 10.8 wt % methane system. In this case the phase transition curves are shifted to very low temperatures. The LCEP is 71.4 °C and 9.33 MPa, more than 65 °C lower than the LCEP of the 13.1 wt % propylene system, and approximately 30 °C lower than the LCEP's for either the carbon dioxide (13.5 wt %) or the ethylene (13.8 wt %) systems. Notice, however, that the vapor pressure curve for this system is at much higher pressures than the vapor pressure curves for any of the three previously mentioned systems.

Shown in Figure 10 are the experimental $P–T$ data for the 11.5 and 13.4 wt % methane systems. The slopes of the LCST curves for these systems are radically different from that for the 10.8 wt % methane system. As the amount of methane added to the polymer solution has increased from 10.8 to 11.4 wt % (and higher), the phase behavior has shifted from that depicted in Figure 1b to that shown in Figure 1c. The additional amount of methane has caused the UCST curve to shift to much
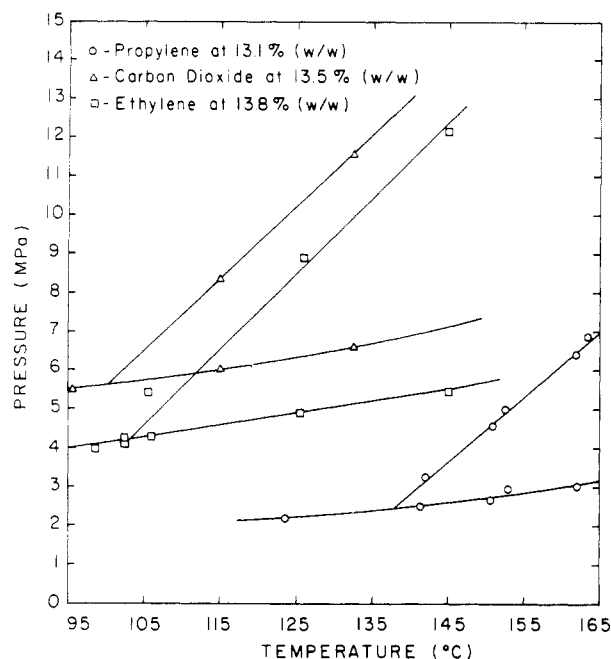
Figure 8. Comparison of the effect of ethylene, propylene, and carbon dioxide on the LCST curve of the EP–solvent system.
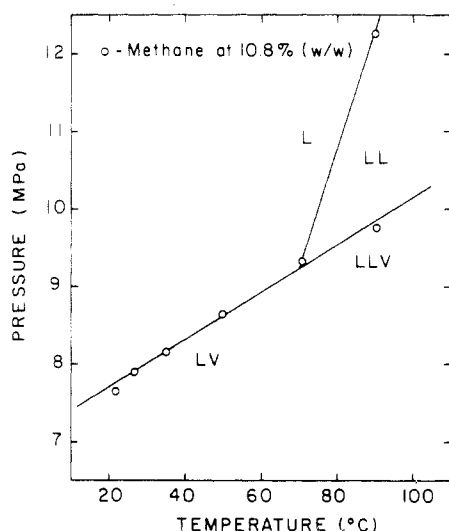

Figure 10. *P–T* projection of the EP–solvent–methane system at methane loadings of 11.5% and 13.4% (w/w).

Figure 9. *P–T* projection of the EP–solvent–methane system at a methane loading of 10.8% (w/w).
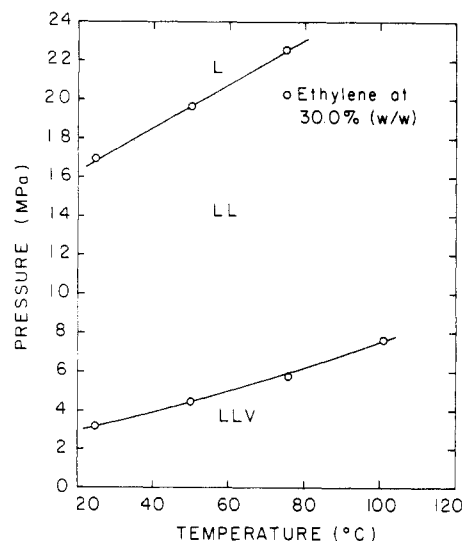
Figure 11. Phase border curves for the EP–solvent–ethylene (30.0% (w/w)) system.

higher temperatures and the LCST curve to shift to lower temperatures until these curves merge into a single curve. Hence, a LL region now exists over a broad range of temperatures and pressures.

The merging of the UCST curve is not unique to the methane system. If the concentration of supercritical additive is increased for the propylene, ethylene, or carbon dioxide system, then these systems would also exhibit the type of phase behavior depicted in Figure 1c. For instance, as the ethylene concentration is increased from 20.0 to 30.0 wt %, the UCST and LCST curves for this system merge, thus resulting in phase behavior which is very similar to the 11.5 and 13.4 wt % methane systems (see Figure 11). The major differences between the methane and ethylene systems are that lower concentrations of methane are needed to merge the UCST and LCST curves while the vapor pressure curves for the methane system are at much higher pressures.

It is interesting that the LCST curve for the 13.4 wt % methane system occurs at much higher pressures than the 11.5 wt % system (see Figure 10). In fact, other qualitative
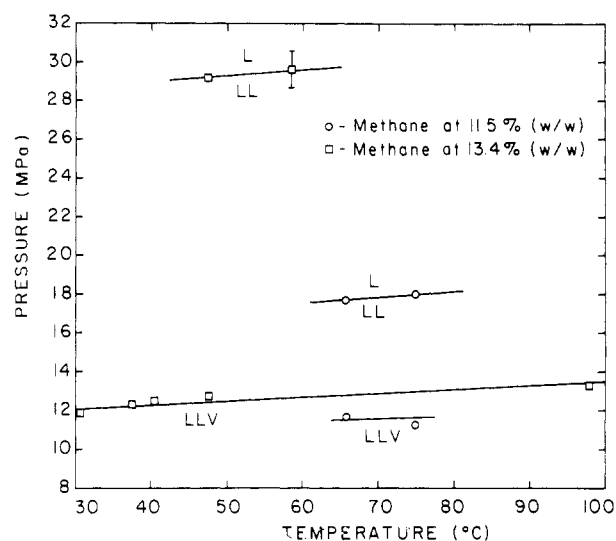
differences are noted between these systems. At 11.5 wt % methane, the heavy liquid phase in the LL region appears gellike, and it occupies approximately $1/3$ the total volume of the view cell. The lighter liquid phase is also grayish and opaque. As the pressure of this system is isothermally increased, the gellike heavy phase remains at approximately $1/3$ the cell volume until the LCST line is crossed and the contents of the cell merge into a single liquid phase. This behavior is similar to that observed for the 30.0 wt % ethylene system.

At 13.4 wt % methane, the heavy liquid phase in the LL region does not have any liquidlike characteristics; it, in fact, looks very stringy. Also, the light liquid phase in this case is very clear and not grayish and opaque as is the case with the other systems previously discussed, including the 11.5 wt % methane systems. This behavior implies that the polymer concentration in the solvent-rich phase is extremely low while the solvent concentration in the polymer-rich phase is also extremely low. As the pressure of the 13.4 wt % system is isothermally increased between pressures of 15 and 24 MPa, the stringy heavy phase tends to coalesce into a ball. When the pressure is increased above 24 MPa, the polymer ball begins to break up and form a thick, gellike liquid phase which now exhibits a meniscus with the lighter, grayish liquid phase. As the

pressure is increased above the LCST curve, the two phases merge into a single clear liquid phase. As expected, hydrostatic pressure converts these methane–solvent mixtures from poor solvents to good solvents.

Discussion

As shown in Figures 5–11 hydrostatic pressure has a dramatic effect on the LCST curve for polymer–solvent systems. This pressure effect is described as

$$[\partial T/\partial P]_c = [\partial^2 \Delta V_{mix}/\partial W_2^2]_c/[\partial^2 \Delta S_{mix}/\partial W_2^2]_c \quad (1)$$

where subscript c denotes the critical curve, W_2 is the weight percent of polymer, and ΔV_{mix} and ΔS_{mix} are the change on mixing of the volume and the entropy, respectively. At the LCST ΔS_{mix} is negative and the rate of change of the curvature of ΔS_{mix} (W_2) is positive, i.e., $[\partial^2 \Delta S_{mix}/\partial W_2^2]_c$ is positive.[18] Patterson has shown that the negative, noncombinatorial contribution to ΔS_{mix} results from a large disparity between the "free volume" (or degree of thermal expansion) of the solvent and the polymer.[9,19] As the pressure is increased isothermally, the free volume of the solvent decreases at a much faster rate than the free volume of the polymer. Finally, at an elevated pressure, the free volume difference between the polymer and its solvent decreases sufficiently to allow these components to become totally miscible. The temperature must be increased to obtain a LCST at this elevated pressure. Therefore, $[\partial T/\partial P]_c$ should be positive along the LCST curve. This qualitative argument is verified for the polymer systems investigated in this study.

The results obtained in this study show that introducing a light SCF additive to the polymer solution causes the LCST curves to shift to lower temperatures. For instance, as shown in Figure 6, a small change in the concentration of ethylene causes a large shift in the LCST curve. The effect of adding an SCF can be understood in terms of the difference in free volume of the mixture components as proposed by Patterson.[20,21] Adding a highly compressible SCF to the polymer solution causes a large disparity between the free volumes of the polymer and the (mixed) solvent. This results in a shift of the LCST curve to lower temperatures, until the LCST curve finally merges with the UCST curve. When the LCST and the UCST curves merge, the resultant critical mixture curve never intersects the solvent vapor pressure curve (see Figure 1c). The effect of the SCF additive is analogous to increasing the molecular weight of the polymer[22] and is opposite to the effect of increasing the pressure on the system.

In an effort to correlate the phase behavior observed in this study the critical temperature of the solvent is used as a measure of the free volume of the solvent. This is in contrast to the approach of Charlet and Delmas,[23] who use solvent density at 25 °C as a measure of the free volume of the solvent. Shown in Figure 12 is a plot of the T-(LCEP) as a function of the critical temperature of the solvent (T_c). For the solvent mixtures used in this study the mixture critical temperature is calculated by using Kay's rule[24]

$$T_{c,mixture} = \sum_{i=1}^{n} x_i T_{ci}$$

where x_i represents the mole fraction of component i in the solvent mixture.

Also plotted on this graph are the LCEP data of Charlet and Delmas[23] for EP–solvent mixtures which consist of an EP polymer of the same molar ethylene content as the EP polymer used here (~53 mol %). Except for a few cases the data are well represented by a single curve. It is surprising that the carbon dioxide system falls reasonably
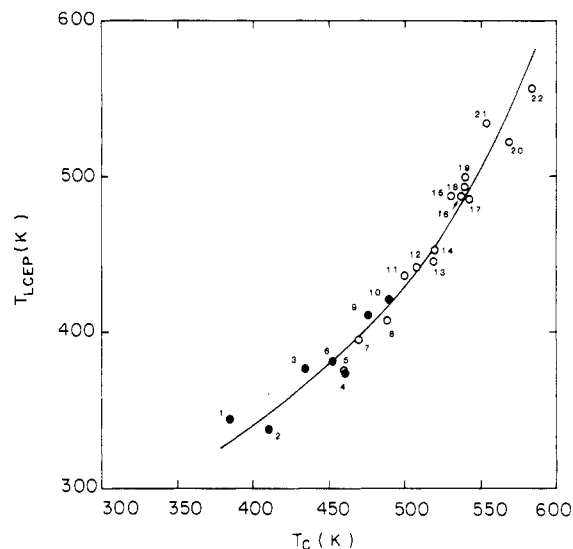

Figure 12. Effect of solvent critical temperature on the LCEP temperature; the shaded circles represent data obtained in this study while the open circles represent data obtained by Charlet and Delmas:[23] (1) 10.8% (w/w) methane system; (2) 20.0% (w/w) ethylene system; (3) 13.8% (w/w) ethylene system; (4) 13.5% (w/w) carbon dioxide system; (5) 2-methylbutane; (6) 9.9% (w/w) ethylene system; (7) n-pentane; (8) 2,2-dimethylbutane; (9) 13.1% (w/w) propylene system; (10) 8.0% (w/w) propylene system; (11) 2,3-dimethylbutane; (12) n-hexane; (13) 2,4-dimethylpentane; (14) 2,2-dimethylpentane; (15) 2,2,3-trimethylbutane; (16) 2,3-dimethylpentane; (17) 2,2,4-trimethylpentane; (18) n-heptane; (19) 3-ethylpentane; (20) n-octane; (21) cyclohexane; (22) 2,3,4-trimethylhexane.

close to the curve since all of the other data are for hydrocarbon solvents. Kay's mixing rule does not distinguish molecular type of solvent and, as such, is not expected to work well for solvent mixtures of hydrocarbons and nonhydrocarbons.

Although the correlating scheme represented in Figure 12 offers the convenience of a straightforward calculational method for estimating T(LCEP), there are a number of limitations to this method. This correlation scheme gives no indication of the pressure at the LCEP. The pressure at the LCEP can be quite high as exhibited by the EP–solvent–methane systems. From the results of this study the pressure at the LCEP (P(LCEP)) increases as the volatility of SCF additive increases (i.e., the P(LCEP) increases in going from propylene to ethylene (which is very close to carbon dioxide) to methane). Quantifying this pressure trend entails using a more fundamental approach to characterizing the experimental data.

The other major limitation of this correlational scheme is that there is no way to estimate the amount of SCF additive needed to merge the LCST and UCST curves. When these curves merge, an LCEP does not exist (e.g., the 11.5 wt % methane system) and, therefore, the correlation scheme fails.

An attempt was made to model the experimental data by using the corresponding states theory of Patterson[21,25] in an effort to predict the trends in the P(LCEP) and the concentration of SCF additive needed to merge the LCST and UCST curves. The mixing rules of Patterson and Delmas[21] are used for the multicomponent solvents investigated in this study. The one adjustable parameter of the model, ν^2 (i.e., ν^2 is a measure of the difference in the chemical nature of the mixture components which affects the location of the UCST and LCST curves), is fitted to the LCEP for each system studied.[25] Unfortunately, physically unrealistic negative values of ν^2 are needed to fit the data. This is more than likely a conse-

quence of the pure-component reduction parameters which are chosen for the SCF additive. These reduction parameters are probably very temperature sensitive. Further modeling work which accounts for the temperature sensitivity of these parameters is being performed for the mixtures investigated in this study.

Conclusion

We have presented new experimental data on the high-pressure phase behavior of various polymer solution–SCF mixtures. The results from this study indicate that adding an SCF additive to a polymer–organic solvent mixture causes the LCST curve to shift to much lower temperatures. In some cases the LCST and UCST curves merge. Hence, polymer can be recovered from solution at very moderate temperatures by introducing an SCF additive to the mixture.

The T(LCEP) can be correlated to the critical temperature of the solvent or SCF solvent mixture. The phase behavior data can also be qualitatively explained by using the corresponding states model of Patterson. Although Patterson's model offers physically satisfying explanations for the phase behavior observed in this study, physically unrealistic values for one of the model parameters are needed to correlate the data. The further attempts are being made to make the model suitable for engineering calculations.

Registry No. methane, 74-82-8; ethylene, 74-85-1; propylene, 115-07-1; carbon dioxide, 124-38-9; (ethylene)·(propylene) (copolymer), 9010-79-1.

Supplementary Material Available: Ten tables of experimental pressure–temperature data (10 pages). Ordering information is given on any current masthead page.

References and Notes

(1) Paulaitis, M. E., Penninger, J. M. L., Gray, R. D., P. Davidson, Eds. "Chemical Engineering at Supercritical Fluid Conditions"; Ann Arbor Science: Ann Arbor, MI, 1983.
(2) Schneider, G. M., Stahl, E., Wilke, G., Eds. "Extraction with Supercritical Gases"; Verlag Chemie: Deerfield Beach, FL 1980.
(3) Gutowski, T. G.; Suh, N. P., paper presented at the 40th Annual Technical Conference of the Society of Plastic Engineers, San Francisco, CA, 1982.
(4) Anolick, C.; Slocum, E. W. U.S. Patent 3 726 843, 1973.
(5) Caywood, S. W. U.S. Patent 3 496 135, 1971.
(6) Anolick, C.; Goffinet, E. P. U.S. Patent 3 553 156, 1971.
(7) Freeman, P. I.; Rowlinson, J. S. *Polymer* **1960**, *1*, 20.
(8) Allen, G.; Baker, C. H. *Polymer* **1965**, *6*, 181.
(9) Zeman, L.; Biros, J.; Patterson, D. *J. Phys. Chem.* **1972**, *76*, 1206.
(10) Irani, C. A.; Cosewith, C; Kasegrande, S. S. U.S. Patent 4 319 021, 1982.
(11) Cowie, J. M. G.; McEwen, I. J. *Macromolecules* **1974**, *7*, 291.
(12) Cowie, J. M. G.; McCrindle, J. T. *Eur. Polym. J.* **1972**, *8*, 1185.
(13) Cowie, J. M. G.; McCrindle, J. T. *Eur. Polym. J.* **1972**, *8*, 1325.
(14) Cowie, J. M. G.; McEwen, I. J. *Polymer* **1983**, *24*, 1449.
(15) McHugh, M. A.; Seckner, A. J.; Yogan, T. J. *Ind. Eng. Chem. Fundam.* **1984**, *23*, 493.
(16) Myrat, C. D.; Rowlinson, J. S. *Polymer* **1965**, *6*, 645.
(17) Rowlinson, J. S.; Swinton, F. L. "Liquids and Liquid Mixtures", 3rd ed.; Butterworth: Boston, MA, 1982.
(18) Prigogine, I.; Defay, R. "Chemical Thermodynamics"; Longmans: London, 1954.
(19) Patterson, D. *Macromolecules* **1969**, *2*, 672.
(20) Zeman, L.; Patterson, D. *J. Phys. Chem.* **1972**, *76*, 1214.
(21) Patterson, D.; Delmas, G. *Trans. Faraday Soc.* **1969**, *65*, 708.
(22) Siow, K. S.; Delmas G.; Patterson, D. *Macromolecules*, **1972**, *5*, 29.
(23) Charlet, G.; Delmas, G. *Polymer* **1981**, *22*, 1181.
(24) Sandler, S. I. "Chemical and Engineering Thermodynamics"; Wiley: New York, 1977.
(25) Zeman, L.; Patterson, D. *J. Phys. Chem.* **1972**, *76*, 1214.

Behavior of Elastomer Networks in Moderately Large Deformations. 1. Elastic Equilibrium[†]

N. W. Tschoegl* and Cigdem Gurer

Division of Chemistry and Chemical Engineering, California Institute of Technology, Pasadena, California 91125. Received March 8, 1984

ABSTRACT: An elastic potential of the form $W = (G_X/2)(\lambda_1{}^2 + \lambda_2{}^2 + \lambda_3{}^2 - 3) + (2G_N/m^2)(\lambda_1{}^m + \lambda_2{}^m + \lambda_3{}^m - 3)$ is proposed, where G_X is the modulus associated with the chemical cross-links of the network, G_N is the modulus contribution arising from the presence of topological constraints, and m can be taken as 0.34. The moduli are linked by the relation $G_X + G_N = G$, where G is the shear modulus. The constitutiveness of this potential is demonstrated on published data in general biaxial deformation of natural rubber. Some of our own data on natural and styrene–butadiene rubber cross-linked to different degrees are also discussed. The nature of G_N has been studied on published data on several different swollen networks.

Introduction

The basic laws of motion, conservation of mass, balance of momenta, conservation of energy, and principle of entropy, valid for all types of continuua, do not form a complete set of equations to describe the response of a material to a mechanical excitation. It is necessary to complement the set with constitutive equations that characterize the material response.

Though largely arbitrary in form, constitutive equations are subject to the restrictions of the constitutive theory.[1] To formulate a constitutive equation valid for all types of materials is a useless task because, due to the generality of such an equation, it would have to contain too many experimentally determined parameters. It is more expedient to group materials into various classes and find a constitutive equation for each class.

Because of their novel characteristics and easy processibility, polymeric materials are being used in increasing

[†]This paper is dedicated to Pierre Thirion on the occasion of his retirement.